European Review for Medical and Pharmacological Sciences 2015; 19: 4603-4609

Visualization of nigrosomes-1 in 3T MR susceptibility weighted imaging and its absence in diagnosing Parkinson's disease

P. GAO[1], P.-Y. ZHOU[2], G. LI[1], G.-B. ZHANG[2], P.-Q. WANG[2], J.-Z. LIU[1], F. XU[1], F. YANG[1], X.-X. WU[1]

[1]Department of Radiology, Xiangyang Hospital Affiliated to Hubei University of Medicine, Xiangyang, Hubei, China
[2]Department of Neurology, Xiangyang Hospital Affiliated to Hubei University of Medicine, Xiangyang, Hubei, China

Ping Gao and Peiyang Zhou contributed equally to this work

Abstract. – OBJECTIVE: To assess the imaging features of nigrosomes-1 in the substantia nigra through 3T MR susceptibility weighted imaging (SWI) and its disease-specific changes for the diagnosis of Parkinson's disease (PD).

PATIENTS AND METHODS: A total of 116 subjects were included in this study and allocated into 3 groups: 54 patients diagnosed with PD were assigned to the PD group, 51 age- and sex-matched volunteers without PD served as the control N-PD group, and 11 clinically suspected PD patients were allocated to the undiagnosed (UD) group. All patients received 3.0T superconducting MRI scanning on xxx. The images were analyzed and compared to assess the ability of nigrosomes-1 signals to depict PD pathology.

RESULTS: The signals of nigrosomes-1 were strong, droplet-like or oval in shape, and were found in 49 patients from the N-PD group (96.08%), on both sides of the SN (47 cases) and unilaterally (2 cases). In contrast, these signals were absent in all 54 cases from the PD group, and were undetected in 7 out of 11 cases in the UD group, 7 cases without the "drop" and 1 case with narrow strips of hyperintensity were clinically proven to PD, 2 cases with the typical hyperintensity were clinically proven to Parkinson's plus syndrome, 2 cases with slightly wider strip of hyperintensity were less sensitive to the drug levodopa.

CONCLUSIONS: The absence of typical droplet-like or oval-shaped nigrosomes-1 signals in 3.0T MR SWI may prove useful in identifying PD and Parkinson's syndrome with high sensitivity and specificity.

Key Words:
Parkinson's disease, Susceptibility weighted imaging, Substantia nigra, Nigrosomes.

Introduction

Parkinson's disease (PD) is a common neurodegenerative disease. The major pathological manifestations of PD are the reduction and loss of striatal dopamine neurons in substantia nigra (SN) and the generation of Lewy bodies in the surviving neurons[1,3]. In 1999, Damier et al[4] discovered a biomarker – "nigrosomes" through pathological section autopsy, which is a small group of dopaminergic cells existing in the healthy SN butlacked in the PD patients. In recent years[5,6] some researchers have applied the susceptibility-weighted imaging (SWI) technique with 7.0T scanner to specimens from healthy people and PD patients. They found that the feature high signals in the normal SN corresponded to the anatomic location of nigrosomes-1, thus realizing the visualization of nigrosomes-1. The purpose of our study was to further analyze the disease-specific imaging changes of nigrosomes-1 through 3.0T SWI, to examine the absence of nigrosomes-1 signals for PD diagnosis, and to explore a neuroimaging method to identify PD and Parkinson's syndrome with high sensitivity and specificity.

Patients and Methods

Patients Information

This study was approved by our hospital Ethics Committee. Signed informed consent forms were obtained from patients before participating.

Materials of the Confirmed Patients

54 hospitalized patients, 33 males and 21 females, aged 48-79 years old (mean 66.2 ± 7.73

Corresponding Author: Guang Li, MD; e-mail: 13597491119@163.com

years old) were diagnosed with PD from June 2012 to May 2014 and assigned to the PD group. Time from symptom onset to admission was 3-12 years (mean 7.72 ± 3.51) years. All patients in the PD group were cognitively evaluated by adopting Mini-mental state examination and the Montreal cognitive assessment. Diagnosis of these patients with PD was confirmed by extrapyramidal disease specialists from the Department of Neurology with reference to the clinical diagnostic criteria established by the think tank of the British Parkinson's Disease Association.

Exclusion criteria: 1) Patients with dementia and other Parkinson's syndrome including Parkinsonism-Plus, essential tremor, and secondary Parkinson's syndrome; 2) Patients with factors affecting the MR image viewed: Motion artifacts heavier, lesions (metal artifacts, old brainstem infarction and hemorrhage) in brainstem.

51 volunteers, 26 male and 25 female, aged 52-77 years old (mean 65.37 ± 9.22 years old) served as the control N-PD group with age, gender, and handedness well matching with the PD groups. This group of participants had no clear clinical symptoms of PD and related medical history. Exclusion criteria referenced to the above.

Newly Admitted Patients with Suspected PD

11 patients with clinically suspected PD were enrolled from June 2014 to November 2014 as the undiagnosed (UD) group, consist of 8 male and 3 female, aged 16-76 years old (mean 60.36 ± 16.16 years old). All of them were also right-handed. Time from symptom onset to admission varied from 0 to 8 years (mean 4.4 ± 2.5 years).

MRI Scanning

The 3.0T superconducting magnetic resonance imaging (MRI) scanners (Signa HDXt, GE, Harvey, IL, USA) were used in this study. Operation parameters include: the channel 8 high-resolution head and neck joint coil as a receiving coil, the axis of the baseline parallel to the direction of corpus callosum. The scanning sequence includes axial SE T2WI (TR 8000 ms, TE 113 ms); T1WI Flair (TR 1814 ms, TE 23.8 ms, TI 860 ms); axial SWI: Oblic 3D Mode, FSPGR, TR/TE: 68.2 ms/6.06, 13.44, 20.81, 28.18, 35.55, 42.92, 50.30, 57.67 ms, 20° flip angle, 2 mm layer thickness, 0mm interlayer spacing, NEX = 1, FOV = 24 mm, matrix 416 × 356, the receiving bandwidth 31.25. The original images were processed by the software Functool in the aw4.6 workstation. The magnitude imaging and phase imaging maps were also acquired.

Image Analysis

Blinded assessment on all MRI images was performed by two senior neuroradiology physicians independently, then got consensus They visually detected the existence of high signals in the nigrosomes-1 section from the SWI magnitude imaging map in patients from each group and then analyzed their characteristics. For those clinically confirmed patients in the PD and N-PD groups (106 cases), after reading the images and reaching an agreement, the two physicians classified them into the N-PD group and the PD group to count. Then, they compared with the clinical gold standards and analyzed the absence of nigrosomes-1 in the use of determining the sensitivity and specificity for PD. Specificity = (cases of visible) / (gold standard of non-PD); sensitivity = (cases of invisible) / (gold standard of PD).

In order to reduce the visual errors, all the images were assessed by the same reader to gather measurement data from the images with relative signals. For patients with typical wedge-shaped high signals in the SN section, measurement was performed at the widest point (a) of the posterolateral wedge-shaped high signal. Width (b) was measured in the midsection of the SN at the same level, and perpendicular to the long axis of the wedge-shaped high signals. The division ratio (a/b) was used to reduce the error due to the difference in the patients' brain capacity.

For those patients with banded high signals in the SN but not typical wedge-shaped high signals, the widest point (c) at the banded high signals was also measured and divided by the middle width of the SN on the same layer to obtain the corresponding ratio (c/b).

Statistical Analysis

Statistical analysis was performed by using the SPSS17.0 (IBM Company, New York, USA) software package. Comparison on gender distribution and age distribution were tested by $\chi 2$ test and independent sample t-test, respectively. Measurable data (a,b,c) and calculated ratio (a/b, c/b) were presented by mean and standard deviation $p < 0.05$ was considered statistically significant.

Images from the 11 subjects in the UD group were subjected to the same analysis procedures. The curative effects were examined according to the corresponding treatment principles.

Table I. Analysis of diagnostic accuracy of nigrosome-1 absence to diagnose PD.

n=105	Physician A		Physician B		Agreement	
	N-PD group	PD group	N-PD group	PD group group	N-PD group	PD group
Unilateral or bilateral visible (cases)	47	0	50	1	49	0
Invisible (cases)	4	54	1	53	2	54
Clinical gold standard (cases)	51	54	51	54	51	54
Lack signs of sensitivity in the diagnosis of PD	100%		98.15%		100%	
Lack signs of specific in the diagnosis of PD	92.16%		98.04%		96.08%	

Two physicians reclassified the clinically diagnosed cases compared with clinical gold standard according to nigrosomes-1 high signal was visible or not in SN. Calculate its sensitivity and specificity.

Results

Imaging Features of Nigrosomes-1 in Confirmed Patients with or Without PD

All analyses were performed in the axial SWI magnitude imaging map where the baseline was parallel to the direction of corpus callosum.

Data of N-PD Group: Strong Nigrosome Signals were Visible in non-PD Patients

Wedge-shaped high signals were visible below the bilateral SN section in the 47 cases in the N-PD group (92.2%). The majority of these signals were droplet-like (Figure 1-A,B), which originated from the fusion of the anteromedial bands and the posterolateral oval structure (Figure 2-B). They were located in the successive 2-3 layers where the red nucleus structure from top to bottom was drawing to a close. The posterolateral oval structure was only shown in 14 cases with very vague front band (Figure 1-C). In 2 other cases, the "droplets" high signals were fully visualized on one side of the SN but unclearly seen on the other side. The other 8 cases had no obvious high signals in the SN on both sides.

We found that the width of the radial line at its widest point of the "droplet", a = 1.22-3.43 mm (mean 2.06 ± 0.54 mm). The width of the band of the high signals perpendicular to the middle SN on the corresponding layer was b = 4.88-7.95 mm (mean 6.74 ± 0.89 mm). a/b = 0.21-0.43 (mean 0.31 ± 0.07 mm) (Figure 3-C).

Data of PD Group: Nigrosome Signals were Absent in PD Patients

In the PD group, the above "droplets" rear oval high signal structures were all absent in 54

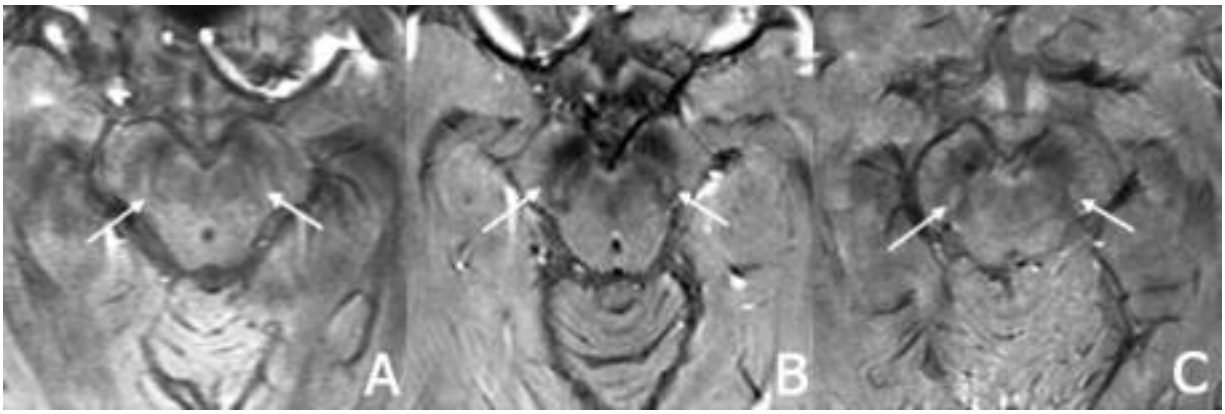

Figure 1. The axial SWI magnitude imaging map of three representative non-PD volunteers. Various shapes of the nigrosomes-1 high signals were marked with white arrows. ***A***, wedge-shaped; ***B***, droplet-like; ***C***, oval. From top to bottom on the layers where the locus ruber disappears, the nigrosomes-1 high signals are all visible in the rear of the SN.

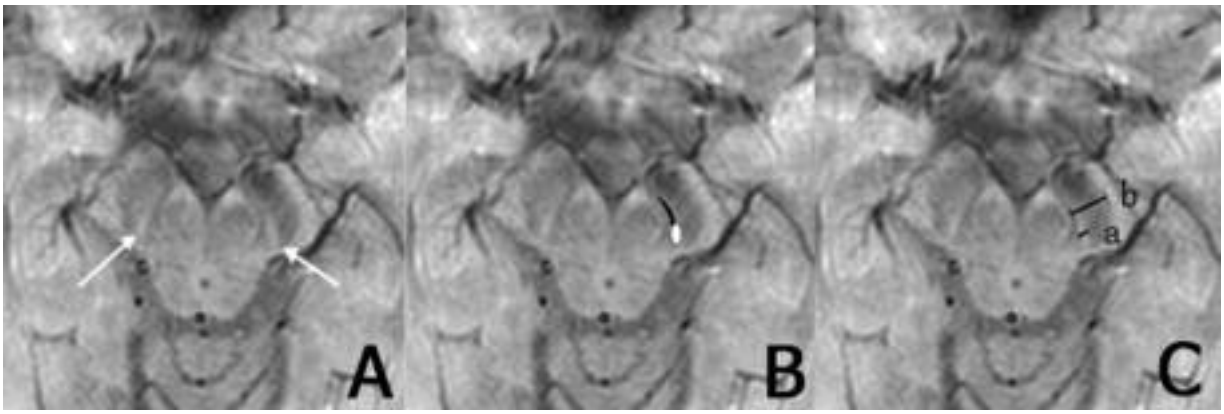

Figure 2. Typical morphology of the nigrosomes-1 high signal in the axial SWI magnitude imaging map of a non-PD volunteer on the same layer and illustration of the measurement methods. ***A,*** nigrosomes-1 high signals in the rear of the healthy SN are "droplet" shaped; ***B,*** the "droplet" consists of posterolateral oval part (marked with white color) and anteromedial banded part (marked with black color); ***C,*** shows the positions of a and b with details: a refers to the widest point of the "droplets" shaped high signals; b refers to the middle width when the SN on this layer is perpendicular to the "droplets" axis.

cases (Figure 3). Among them, 35 cases were characterized as complete absence of "droplets" high signals and these patients showed relatively high sensitivity to levodopa drugs at conventional doses. Moreover, the thin-banded high signals were faintly visible on one side in the 13 other cases and on both sides in the remaining 6 cases. The width at its widest point of the banded high signals (c), was 1.13 mm-1.32 mm (mean 1.22 ± 0.05 mm). In the corresponding layer, the middle width in the SN section (*b*) was 4.90 mm-7.51 mm (mean 6.69 ± 0.73 mm). The ratio of *c*/*b* was 0.15 mm-0.25 mm (mean 0.19 ± 0.03 mm).

Comparison Between N-PD and PD Groups

Two physicians reclassified patients compared with clinical gold standard according to nigrosomes-1 high signal was visible or not in SN (Table I). Results from the PD group and the N-PD group suggested that the absence of high signals in the nigrosomes-1 section can evaluate the sensitivity of PD amounts to 100% while specificity about 96.08%. χ^2 test was used according to the signs of "yes", "no" classification. The result was $p = 0.000<0.05$ bilateral. The differences were statistically significant.

Nigrosome Imaging as a Diagnostic Test for Unconfirmed Patients Experimental Diagnoses for the Unconfirmed Patients and the Treatment Effects

Among the 11 cases in the UD group, 9 cases lacked the structure of the above "droplets" rear oval high signals. Among these 9 cases,

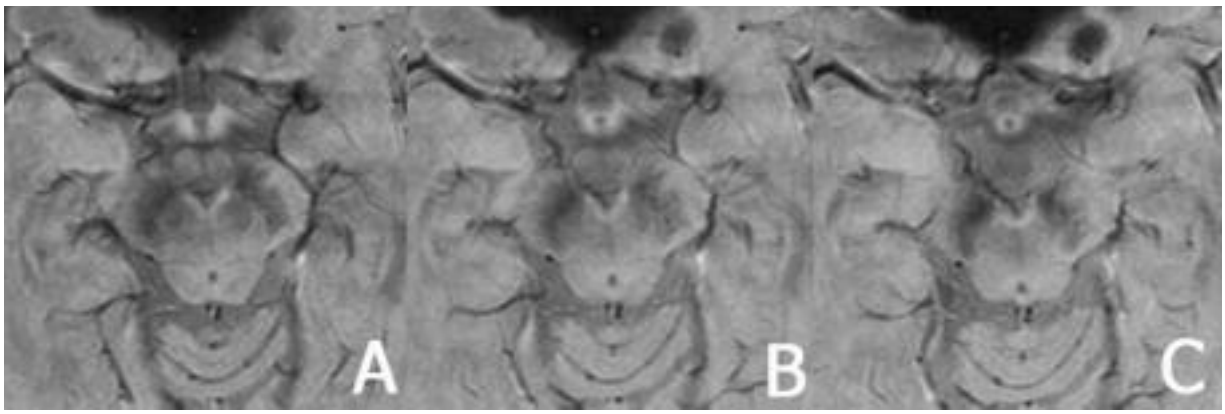

Figure 3. Imaging performance at the corresponding level of the SN in PD. The axial SWI magnitude imaging map of the same PD patient: Nigrosomes-1 high signals are absent on the continuous three layers in the corresponding area.

"droplets-shaped" high signals were completely absent in 6 cases, who displayed relatively high sensitivity to levodopa drugs with conventional doses. In another 2 cases, banded high signals can be seen on the one side while there was 1 case where the banded high signals were visible on both sides. The widths at their widest point of the banded high signals (*c*) were = 1.12 mm, 1.29 mm, and 1.58 mm, respectively. The latter two cases showed poor sensitivity to levodopa drugs with conventional doses, so we had to repeatedly add doses to them so as to maintain curative effects. The ratio between them and the width of the middle part in the SN section in their corresponding layer is about $c/b = 0.23$ and 0.31.

For the 2 cases whose "droplets" high signals still existed, through MR scanning images and related medical history, they were patients with olivopontocerebellar atrophy (16 years old) and progressive supranuclear paralysis (47 years old), respectively. When they received experimental treatment with levodopa drugs, the result is not very effective.

Discussion

PD is a common neurodegenerative disorder among middle-aged and elderly people, resulting from degeneration of dopaminergic neurons in the SN of midbrain. Significant reduction in the content of dopamine in striatum and the appearance of Lewy bodies in the SN and LC may cause the dysfunction of basal ganglia and cortical circuits[7-11]. Fearnley et al[12] found that long before the subjective symptom in movement appeared, 60% to 80% loss of the corresponding neurons was already found in PD patients.

In 1999, Damier et al[4] discovered a new type of PD biological marker through autopsy pathological section, Nigrosomes.which is a small group of dopaminergic cells in the substantia nigra and partially pigment-free in the immunohistochemical staining of the calcium antagonist protein D28K for healthy people. While it's absent in the substantia nigra and can be stained in the immunohistochemical staining for PD patients. Nigrosomes consist of 5 families, among which nigrosomes-1 is the largest. Though nigrosomes-1 only covers an area of a few millimeters, as many as 98% of the dopaminergic cells are depleted in this area in PD patients[13,14].

SWI is a type of T2* pulse sequencing technique recently developed in the field of MRI. It detects the susceptibility differences between tissues in the magnetic field to produce an enhanced MRI contrast. Compared with the traditional MRI imaging techniques, SWI uses 3D gradient echo scanning, a fully velocity compensation, and the RF spoiled technology[16-18]. It features three dimensions, high-resolution and high signal to noise ratio. Its imaging principle is that substances such as fat, iron, calcium, deoxyhemoglobin have different magnetic susceptibilities from their neighboring tissues so as to cause uneven local magnetic fields to manifest the distribution of the brain iron[19-21]. Compared with T2WI, SWI has stronger magnetic sensitivity, adopts thinner layer thickness and no-interval scanning, so it can show the SN pars compacta and pars reticulata as well as the form and structure of locus ruber more clearly; thus, more accurate measurement data can be acquired.

In 2013, Blazejewska et al[5] applied SWI to specimens of healthy people and PD patients through using superconducting 7.0T and 3.0T MRI scanner. The result shows that ovoid high signals are visible in the posterolateral SN pars compacta under the two kinds of scanning, corresponding to the missing position of the nigrosomes-1 immunohistochemical staining. However, among PD patients, the ovoid high signals are absent, realizing the visualization of nigrosomes-1. In 2014, Cosottini et al[6], further discovered that in the 7.0T SWI images, the normal SN structure can clearly manifest 7 layers under the environment of 7T. The C1 area in the C layer is equivalent to the missing position of the nigrosomes-1 immunohistochemical staining in the form of droplets-shaped high signals. But the strong electromagnetic radiation of the 7.0T scanner in terms of biological effects on the living body cannot be ignored[22-26]. This is the reason why this method cannot be widely applied in clinic. With the popularization of 3.0T magnetic resonance in clinic[27-29], we can try to conduct related research on the living body under this circumstance.

Our study showed several important findings. On the axial SWI magnitude imaging map where the baseline is parallel to the direction of corpus callosum, the SN pars compacta of those non-PD patients corresponds to the feature high signals in the nigrosomes-1 which is mostly like "droplets" or "pause" (Figure 1 A, B, Figure 2 A), formed by the combination of anteromedial banded and posterolateral oval structures (Figure 2 B), but part of them only show the posterolateral oval ar-

eas (Figure 1 C). The average width at its widest point of the oval high signal is about (2.06 ± 0.54 mm), and its average ratio with the width in the middle of the SN in the corresponding layer is about (0.31 ± 0.07 mm). This special signal is located in the continuous 2-3 layers of the locus ruber structure which is coming to an end from top to bottom. In the corresponding areas of the PD patients, the high signals are basically absent (Figure 3).

The absence of high signals is used to evaluate the sensitivity and specificity in the PD diagnosis which are 100% and around 96.08%, respectively. Motion artifacts, metal artifacts, and other lesions in the brain stem have a profound impact on observing the signals, so before scanning we need to remove metal accessories and in the process of scanning, it is necessary to adjust the head and neck of patients, which are crucial to improve the accuracy of diagnosis.

In the UD group, 6 out of 11 cases completely lost "droplets-shaped" high signals. 1 case showed narrow banded high signals on both sides. These patients demonstrated high susceptibilities to levodopa drugs. These results indicate that PD diagnosed with "droplets" high signals missing had a certain feasible.

In the UD group, there were 2 cases with "droplets" high signals. By examining the MR scanning images and related medical history, we considered them to be olivopontocerebellar atrophy and progressive supranuclear paralysis, respectively. Two cases with relatively broad-banded high signals had poor sensitivity to levodopa drugs and their curative effects cannot last long. Perhaps they were other type of Parkinson's syndrome. For patients with Parkinson's typical symptoms in clinic, the existence of "droplets-shaped" high signals in the SN and their width was likely to be an effective method to identify PD and Parkinson's syndrome. But as in this group related samples were very few, it was necessary to accumulate more to get more accurate results.

Conclusions

On the 3.0T MR SWI, typical "droplets-shaped" or oval high signals can be observed in the nigrosomes-1 area in the SN of the non-PD patients. The absence of nigrosome-1 high signals in 3T MR susceptibility weighted imaging might prove useful in developing a relatively simple and reliable diagnostic test for PD. Further research is the accumulation of more cases to confirm the clinical role of this phenomenon in the identification of PD and Parkinson's syndrome.

Conflict of Interest

The Authors declare that they have no conflict of interests.

References

1) Cao HY, Zhang MM. Advances of the Brain imaging findings in Parkinson's disease with MRI. Chinese J of Radiol 2010; 44: 332-334.
2) Zhu RL, Lu XC, Tang LJ, Huang BS, Yu W, Li S, Li LX. Association between HLA rs3129882 polymorphism and Parkinson's disease: a meta-analysis. Eur Rev Med Pharmacol Sci 2015; 19: 423-432.
3) Zou YM, Tan JP, Li N, Yang JS, Yu BC, Yu JM, Du W, Zhang WJ, Cui LQ, Wang QS, Xia XN, Li JJ, Zhou PY, Zhang BH, Liu ZY, Zhang SG, Sun LY, Liu N, Deng RX, Ma LH, Chen WJ, Zhang YQ, Liu J, Zhang SM, Lan XY, Zhao YM, Wang LN. The prevalence of Parkinson's disease continues to rise after 80 years of age: a cross-sectional study of Chinese veterans. Eur Rev Med Pharmacol Sci 2014;18: 3908–3915.
4) Damier P, Hirsch EC, Agid Y, Graybiel AM. The substantia nigra of the human brain. I. Nigrosomes and the nigral matrix, a compartmental organization based on calbindin D(28K) immunohistochemistry. Brain 1999; 122: 1421-1436.
5) Mueller C, Pinter B, Reiter E, Schocke M, Scherfler C, Poewe W, Seppi K, Blazejewska AI, Schwarz ST, Bajaj N, Auer DP, Gowland PA. Visualization of nigrosome 1 and its loss in PD: pathoanatomical correlation and in vivo 7T MRI. Neurology 2014; 82: 1752.
6) Cosottini M, Frosini D, Pesaresi I, Costagli M, Biagi L, Ceravolo R, Bonuccelli U, Tosetti M. MR imaging of the substantia nigra at 7T enables diagnosis of Parkinson disease. Radiology 2014; 271: 831-838.
7) Altinayar S, Oner S, Can S, Kizilay A, Kamisli S, Sarac K. Olfactory dysfunction and its relation olfactory bulb volume in Parkinson's disease. Eur Rev Med Pharmacol Sci 2014; 18: 3659-3664.
8) Jost WH, Friede M, Schnitker J. Comparative efficacy of selegiline versus rasagiline in the treatment of early Parkinson's disease. Eur Rev Med Pharmacol Sci 2014; 18: 3349.
9) Wu SF, Zhu ZF, Kong Y, Zhang HP, Zhou GQ, Jiang QT, Meng XP. Assessment of cerebral iron content in patients with Parkinson's disease by the susceptibility-weighted MRI. Eur Rev Med Pharmacol Sci 2014; 18: 2605-2608.

10) Yu X, Wang F, Zhang JP. Meta-analysis of the association of rs7702187 SNP in SEMA5A gene with risk of Parkinson's disease. Eur Rev Med Pharmacol Sci 2014; 18: 900-904.

11) Olanow CW, McNaught K. Parkinson's disease, proteins, and prions: milestones. Mov Disord 2011; 26: 1056-1071.

12) Fearnley JM, Lees AJ. Ageing and Parkinson's disease: substantia nigra regional selectivity. Brain J Neurol 1991; 114: 2283-2301.

13) Kouti L, Noroozian M, Akhondzadeh S, Abdollahi M, Javadi MR, Faramarzi MA, Mousavi S, Ghaeli P. Nitric oxide and peroxynitrite serum levels in Parkinson's disease: correlation of oxidative stress and the severity of the disease. Eur Rev Med Pharmacol Sci 2013; 17: 964-970.

14) Fasano A, Ricciardi L, Lena F, Bentivoglio AR, Modugno N. Intrajejunal levodopa infusion in advanced Parkinson's disease: long-term effects on motor and non-motor symptoms and impact on patient's and caregiver's quality of life. Eur Rev Med Pharmacol Sci 2012; 16: 79-89.

15) Sanyal J, Bandyopadhyay SK, Banerjee TK, Mukherjee SC, Chakraborty DP, Ray BC, Rao VR. Plasma levels of lipid peroxides in patients with Parkinson's disease. Eur Rev Med Pharmacol Sci 2009; 13: 129-132.

16) Bulut HT, Sarica MA, Baykan AH. The value of susceptibility weighted magnetic resonance imaging in evaluation of patients with familial cerebral cavernous angioma. Int J Clin Exp Med 2014; 17: 5296-5302.

17) Agarwal A, Vijay K, Thamburaj K, Kanekar S, Kalapos P. Sensitivity of 3D gradient recalled echo susceptibility-weighted imaging technique compared to computed tomography angiography for detection of middle cerebral artery thrombus in acute stroke. Neurol Int 2014; 6: 5521-5532.

18) Ryan NP, Catroppa C, Cooper JM, Beare R, Ditchfield M, Coleman L, Silk T, Crossley L, Rogers K, Beauchamp MH, Yeates KO, Anderson VA. Relationships between acute imaging biomarkers and theory of mind impairment in post-acute pediatric traumatic brain injury: A prospective analysis using susceptibility weighted imaging (SWI). Neuropsychologia 2015; 66: 32-38.

19) Haacke EM, Cheng NY, House MJ, Liu Q, Neelavalli J, Ogg RJ, Khan A, Ayaz M, Kirsch W, Obenaus A. Imaging iron stores in the brain using magnetic resonance imaging. Magn Reson Imaging 2005; 23: 1-25.

20) Sehgal V, Delproposto Z, Haacke EM, Tong KA, Wycliffe N, Kido DK, Xu Y, Neelavalli J, Haddar D, Reichenbach JR. Clinical applications of neuroimaging with susceptibility-weighted imaging. J Magn Reson Imaging 2005; 22: 439-450.

21) Mehemed TM, Yamamoto A, Okada T, Kanagaki M, Sawada T, Morimoto E, Takahashi JC, Miyamoto S, Togashi K. Analysis of susceptibility-weighted images of cortico-medullary junction. Magn Reson Med Sci 2014; 13: 231-238.

22) Zhang Z, Liao W, Bernhardt B, Wang Z, Sun K, Yang F, Liu Y, Lu G. Brain iron redistribution in mesial temporal lobe epilepsy: a susceptibility-weighted magnetic resonance imaging study. BMC Neurosci 2014; 15: 117.

23) Zhang XT, Liu J, Schmitter S, Van de Moortele PF, Bin HE. Predicting temperature increase through local SAR estimation by B1 mapping: a phantom validation at 7T. Conf Proc IEEE Eng Med Biol Soc; 2014: 1107-1110.

24) By S, Rispoli JV, Cheshkov S, Dimitrov I, Cui J, Seiler S, Goudreau S, Malloy C, Wright SM, McDougall MP. A 16-channel receive, forced current excitation dual-transmit coil for breast imaging at 7T. PLoS One 2014; 24; 9: e113969.

25) Zhao Y, Zhao T, Raval SB, Krishnamurthy N, Zheng H, Harris CT, Handler WB, Chronik BA, Ibrahim TS. Dual optimization method of radiofrequency and quasistatic field simulations for reduction of eddy currents generated on 7T radiofrequency coil shielding. Magn Reson Med 2015; 74: 1461-1469.

26) Thai CT, Karam IM, Nguyen-Thi PL, Lefèvre F, Hubert J, Felblinger J, Eschwège P. Pelvic magnetic resonance imaging angioanatomy of the arterial blood supply to the penis in suspected prostate cancer patients. Eur J Radiol 2015; 84: 823-827.

27) Teichtahl AJ, Smith S, Wang Y, Wluka AE, O Sullivan R, Giles GG, Cicuttini FM. Occupational risk factors for hip osteoarthritis are associated with early hip structural abnormalities: a 3.0T magnetic resonance imaging study of community-based adults. Arthritis Res Ther 2015; 17: 19.

28) Li Y, Wang E, Han X, Gao L, Zheng M, Zhang Y, Ren T, He G, Yan X, Zheng H, Xue Z. Default mode network in childhood absence epilepsy by 3.0T magnetic resonance imaging. Zhonghua Yi XueZaZhi 2014; 94: 3540-3544.

29) Snoussi K, Gillen JS, Horska A, Puts NA, Pradhan S, Edden RA, Barker PB. Comparison of brain gray and white matter macromolecule resonances at 3 and 7 Tesla. Magn Reson Med 2015; 74: 607-613.